JACS
JOURNAL OF THE AMERICAN CHEMICAL SOCIETY

Communication

Iridium-catalyzed Asymmetric Borylation of Unactivated Methylene C(sp)–H Bonds

Ronald L. Reyes, Tomohiro Iwai, Satoshi Maeda, and Masaya Sawamura

J. Am. Chem. Soc., **Just Accepted Manuscript** • DOI: 10.1021/jacs.9b01952 • Publication Date (Web): 15 Apr 2019

ACS Publications

is published by the American Chemical Society. 1155 Sixteenth Street N.W., Washington, DC 20036

Iridium-catalyzed Asymmetric Borylation of Unactivated Methylene C(sp^3)–H Bonds

Ronald L. Reyes,[1,2] Tomohiro Iwai,[1] Satoshi Maeda,[1,2,*] and Masaya Sawamura[1,2,*]

[1] Department of Chemistry, Faculty of Science, Hokkaido University, Sapporo 060-0810, Japan

[2] Institute for Chemical Reaction Design and Discovery (WPI-ICReDD), Hokkaido University, Sapporo 001-0021, Japan

Supporting Information Placeholder

ABSTRACT: Herein, we show the highly enantioselective borylation of unactivated methylene C(sp^3)–H bonds in 2-alkylpyridines and 2-alkyl-1,3-azole derivatives using an iridium-BINOL-based chiral monophosphite catalyst system. Quantum chemical calculations using the artificial force induced reaction (AFIR) method suggested that a monophosphite-Ir-tris(boryl) complex generates a narrow chiral reaction pocket where the differentiation of the enantiotopic methylene C–H bonds is accomplished through an assembly of multiple noncovalent interactions.

Transformative synthetic strategies that circumvent challenges in the activation of C(sp^3)–H bonds remain underdeveloped despite the significant advances in recent years.[1] A common theme in asymmetric C(sp^3)–H activation involves the inception of chirality by the desymmetrization of symmetrical molecules through differentiation of enantiotopic carbons that leads to an array of stereochemistry-generating C–H functionalization (Figure 1a).[2] A more challenging stereocenter-generating transformation involves the discrimination of enantiotopic C(sp^3)–H bonds situated on a single methylene carbon center (Figure 1b). While a greater number of reports exist on transformations of considerably activated methylene C–H bonds located α-to-heteroatoms[3] or at benzylic positions,[4] asymmetric discrimination of unactivated enantiotopic methylene C–H bonds is relatively rare and has been a long-standing challenge in organic synthesis. Successful strategies in this area include mechanistically outer sphere processes[5] and inner-sphere asymmetric C(sp^3)–H cleavage through a concerted metalation-deprotonation pathway.[6]

We previously described the heteroatom-directed borylation of unactivated methylene C(sp^3)–H bonds by employing a heterogeneous Ir-catalyst system based on silica-supported monophosphine ligand, Silica-SMAP (Figure 1c).[7] The 1:1 metal/P ratio and the proximity effect due to the heteroatom-to-metal coordination are both indispensable to allow the efficient site-selective borylation of C–H bonds situated γ to the heteroatom in the directing group. Significantly, we found that some soluble homogeneous monophosphines including chiral phosphoramidite ligands can also promote these transformations with moderate enantioselectivities.[8,9]

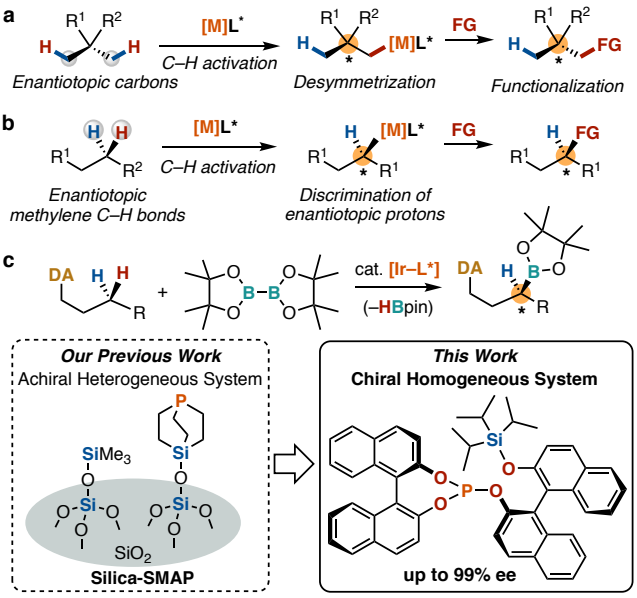

Figure 1. C(sp^3)–H bond activation strategies featuring the desymmetrization of enantiotopic carbons (a) or by the differentiation of enantiotopic methylene C–H bonds (b). (c) Site-selective borylation of methylene C(sp^3)–H bonds by the achiral or chiral Ir-catalyst systems. FG: Functional group; DA: Donor atom.

Encouraged by the preliminary outcome, we investigated the readily modifiable monophosphite family (Figure 2). Simple atropisomeric BINOL-based monophosphite bearing an unsubstituted phenolic moiety **L1** for the borylation of 2-propylpyridine (**1a**) with bis(pinacolato)diboron (**2**) under iridium catalysis [**1a**/**2** 2:1, Ir: 3 mol %, Ir/P 1:1, cyclopentyl methyl ether (CPME) as a solvent, 80 °C, 15 h] followed by oxidation of the corresponding secondary alkylboronate **3a** showed an inadequate performance. Modifications to the phenolic moiety at the two ortho-positions with Me

groups (**L2**) resulted in limited reactivity and low enantioselectivity. In contrast, the enantioselectivity was significantly improved when Ph groups were introduced instead (**L3**). Homologous P-substitution by a 1-naphthol moiety (**L4**) further enhanced the enantioselectivity up to 76% ee, pointing out an intuitive trend favoring an extended aromatic environment. This prompted us to introduce a second BINOL group. To our satisfaction, the reported phosphite **L5**[10] delivered the product at 80% ee. Furthermore, the modification of the OH group with a TIPS group produced even better performing ligand **L6**, leading to a jump up of enantioselectivity to 90% ee, despite the formation of undesired pyridyl C(sp^2)–H borylation products (9%).

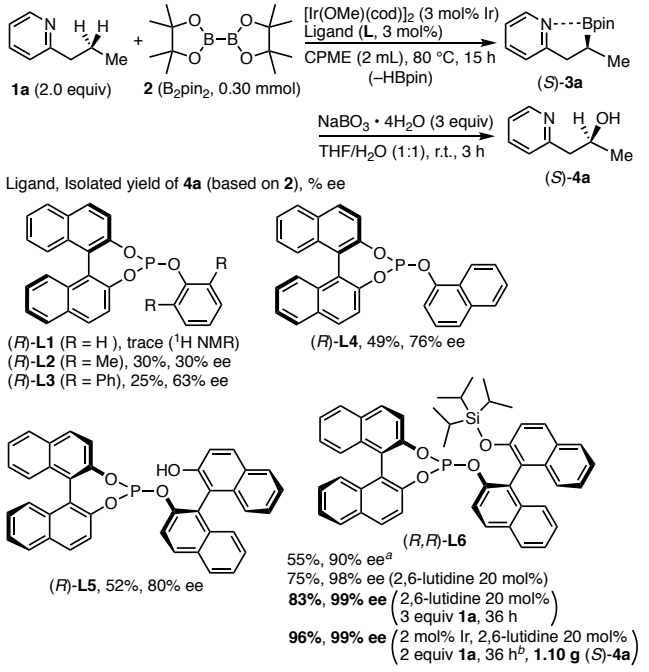

Figure 2. Ligand effects in the Ir-catalyzed asymmetric borylation of **1a**. Borylation conditions: **1a** (0.60 mmol), **2** (0.30 mmol), [Ir(OMe)(cod)]$_2$ (Ir: 3 mol%), **L1-6** (3 mol%), CPME (2 mL), 80 °C, 15 h. Oxidation conditions: $NaBO_3 \cdot 4H_2O$ (0.90 mmol), THF (1 mL), H_2O (1 mL), r.t., 3 h, open air. [a] C(sp^2)–H borylation product (9%) was observed. [b] Gram-scale reaction: **1a** (16.5 mmol), **2** (8.25 mmol), [Ir(OMe)(cod)]$_2$ (Ir: 2 mol%), (*R*,*R*)-**L6** (2 mol%), 2,6-lutidine (20 mol%), CPME (10 mL), 80 °C, 36 h.

Interestingly, the use of 2,6-lutidine (20 mol%) as an additive was effective in not only suppressing the pyridine ring borylation but also increasing the enantioselectivity, giving **4a** as the sole product in 75% yield at 98% ee (see Figure 2). This result was further enhanced by using 3 equiv of **1a** in the presence of 20 mol% of 2,6-lutidine, isolating the product in 83% yield at 99% ee.[11, 12] The protocol is also applicable at a larger scale (2 mol% Ir-**L6** cat., **1a** 2eq). The absolute configuration of **4a** was determined to be *S* by comparing its optical rotation with the literature value.[13]

Next, we investigated the substrate scope (Table 1). Thus, 2-pentylpyridine underwent the enantioselective borylation-oxidation reaction to give the corresponding product **4b** (96% ee, entry 1). The presence of both electron-donating and electron-withdrawing groups at the pyridyl moiety were tolerated to give products **4c** and **4d** with excellent enantioselectivities of 94% ee and 97% ee, respectively (entries 2 and 3). The borylation of 2-(3-phenylpropyl)pyridine occurred with exclusive site selectivity giving **4e** (93% ee) in 75% yield (entry 4).

Table 1. Ir-catalyzed asymmetric borylation of methylene C(sp^3)–H bonds (Scope of the borylation-oxidation protocol).[a]

entry	oxidation product **4**		yield of **4** (%)[b]	ee of **4** (%)[c]
1[d]	**4b**	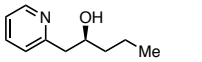	87	96 (*S*)
2[d]	**4c**	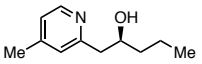	85	94 (*S*)
3[d, e]	**4d**	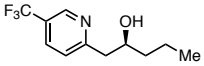	65	97 (*S*)
4	**4e**	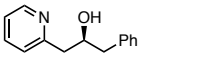	75	93 (*S*)
5	**4f**	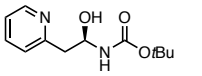	54	91 (*R*)
6[d]	**4g**	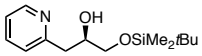	52	95 (*R*)
7	**4h**	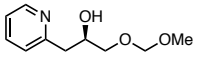	78	94 (*R*)
8[d]	**4i**	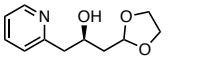	53	92 (*R*)
9[e]	**4j**	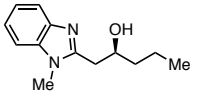	95	93 (*S*)
10	**4k**	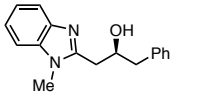	86	98 (*S*)
11[e]	**4l**	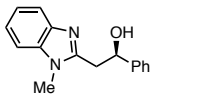	75	96 (*R*)
12[d]	**4m**	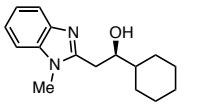	87	95 (*R*)
13[d, e]	**4n**	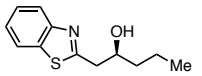	87	92 (*S*)
14[d]	**4o**	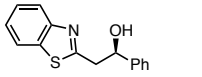	71	92 (*R*)
15[d, e]	**4p**	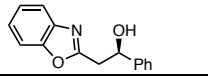	78	90 (*R*)

[a] Borylation conditions: **1** (0.90 mmol, 3 equiv), **2** (0.30 mmol), [Ir(OMe)(cod)]$_2$ (3 mol% Ir), (*R*,*R*)-**L6** (3 mol%), CPME (2 mL), 80 °C, 15 h. Oxidation conditions: $NaBO_3 \cdot 4H_2O$ (0.90 mmol), THF (1 mL), H_2O (1 mL), r.t., 3 h. [b] Isolated yield of **4** based on **2**. [c] Enantiomeric excess (ee) was determined by chiral HPLC analysis. [d] 20 mol% of

2,6-lutidine was used as an additive. [e] The borylation was conducted for 24 h.

An *N*-Boc-aminoalkyl substrate allowed the borylation of a C(sp^3)–H at the position γ to the pyridine N atom and adjacent to the N atom of the secondary amino group, giving the enantioenriched α-*N*-Boc-amino alcohol **4f** (91% ee, Table 1, entry 5). Substrates with a silyl- or MOM-protected hydroxyl group also gave the corresponding enantioenriched products **4g** (95% ee) or **4h** (94% ee), respectively (entries 6 and 7). The reaction of a substrate possessing a cyclic acetal moiety occurred cleanly to give **4i** (92% ee) (entry 8).

Other 2-alkylheteroaryl derivatives were suitable substrates. The C(sp^3)–H borylation of benzimidazole derivatives occurred efficiently with exclusive site selectivity, giving **4j** and **4k** at excellent enantioselectivities (Table 1, entries 9 and 10). The borylation of more congested 2-(2-phenylethyl)benzimidazole or the corresponding cyclohexyl-substituted substrate also proceeded smoothly with excellent enantioselectivities (**4l**, 96% ee, **4m**, 95% ee, entries 11 and 12), demonstrating a significant tolerance of this protocol toward steric hindrance. Other benzo-fused substrates including benzothiazole and benzoxazole derivatives also gave the enantioenriched alcohols **4m–p** with high enantioselectivities (entries 13–15).

Kinetic analysis using **1a** or 2-(2,2,3,3,3-pentadeuterioprop-1-yl)pyridine (**1a**-d_5) with **2** and the Ir-**L6** catalyst system gave a significant kinetic isotope effect value, k_H/k_D = 3.6. This value implied that a turnover-limiting step of the Ir catalysis involved the cleavage of a C(sp^3)–H bond (see Supporting Information for details of the kinetic studies).[14] Based on this result, we conducted preliminary quantum chemical calculations, focusing on C–H bond cleavage by the catalyst. Considering an ambiguity and difficulty in locating appropriate transition states (TS) for a large-scale full reaction system with standard DFT methods, we employed the artificial force induced reaction (AFIR) method implemented in the GRRM program.[15,16] For an initial setup, we explored the conformations of **L6** using the single-component mode of the AFIR method (SC-AFIR), which generated a total of 93 conformers.

Among them, the 10 lowest energy conformers were selected for the three-component complexation with Ir(Bpin)$_3$ and 2-propylpyridine (**1a**) under artificial forces in the multi-component mode (MC-AFIR). This led to the finding of a reasonable P,N-coordinated precursor Ir complex that exhibited an agostic interaction between the *pro-S* hydrogen atom γ to the pyridine N atom and the Ir(III) center. Then, **1a** was relocated manually at the Ir coordination sphere for interchanges of enantiotopic C–H bonds and N/C–H coordination sites for following SC-AFIR searches that explore four (2x2) approximate transition states (apprTSs). Then, the same workflow was applied for other two **L6**-Ir(Bpin)$_3$ backbone structures produced manually through the rotation of the Ir–P bond (ca. 120° and 240°). The resulting twelve (2x2x3) apprTSs were fully optimized without artificial force using M06-L density functional including D3 empirical dispersion correction (SDD for Ir, 6-31G*). The IRC analysis was then conducted for all of the DFT-optimized TSs.[17] Finally, single point energy calculations were done using MN15 density functional [SMD (Et_2O), SDD for Ir, 6-311G(2d,p)].

Chemical diagrams and relative free energies of the optimized local minima (**PC-*S*** and **PD-*S***) and transition states (**TS-*S***) for the C(sp^3)–H bond cleavage reaction pathway that goes through the most stable TS (**PC-*S***–**TS-*S***–**PD-*S***) with an energy barrier of 23.8 kcal mol^{-1} is shown in Figure 3. The precursor complex (**PC-*S***) has a C–H···Ir(III) agostic interaction and the product complex (**PD-*S***) has the Ir(V) center σ-bonded to the C(sp^3) and H atoms, indicating that this step is a concerted C(sp^3)–H bond oxidative addition to the Ir(III) center.

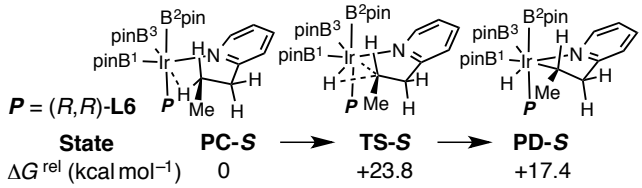

Figure 3. Chemical diagrams and relative free energies of the DFT-optimized local minima (**PC-*S***) and **PD-*S***) and transition states (**TS-*S***) for the most favorable C(sp^3)–H bond cleavage reaction pathway.

Three-dimensional representations with important geometrical features of the most stable *S*-producing TS (**TS-*S***) are shown in Figure 4a in comparison with those of the most relevant *R*-producing TS (**TS-*R***) (Figure 4b). The former is 2.8 kcal mol^{-1} lower in energy than the latter at 80 °C.[18] The **L6**-Ir(Bpin)$_3$ backbones are virtually superimposable between the two TSs (Figure S8). Thus, this comparison should be useful to discuss how the catalyst in the specific conformation is able to differentiate the enantiotopic C(sp^3)–H bonds. The bulky TIPS group fills a space on the backside of the P lone pair, making the silyloxy-substituted naphthalene ring stand upward approaching the Ir(Bpin)$_3$ site. As a result, two of the ligand naphthalene rings and the three Bpin groups produce a narrow chiral reaction pocket with the deeply embedded Ir center, in which the 2-alkylpyridine substrate, in either **TS-*S*** or **TS-*R***, is accommodated not only through metal-centered coordination but also with the assembly of weak attractive interactions such as π/π, C–H/π, and C–H···O interactions.[19–21]

Mapping of noncovalent interaction surfaces by NCIPlot and VMD analysis visualizes stabilizing effects within the reaction pocket (Figure 4).[22,23] The pyridine ring and the naphthalene ring are stacked to each other in the more stable **TS-*S***, while they are more angular in

TS-*R*. Thus, the former has more gain of stabilization energy in terms of π/π interactions. In addition, stabilization of **TS-*S*** by C–H/π interactions is significant between the pyridine moiety and a methyl group of the B^2pin moiety, while such interactions are present only in a diminished magnitude in **TS-*R***. Moreover, non-classical hydrogen bonds that occur between C(sp^3)–H or C(sp^2)–H bonds in the substrate and O atoms presented in the surface of the catalytic pocket may also contribute to the difference in stability between the two TSs.[19–21]

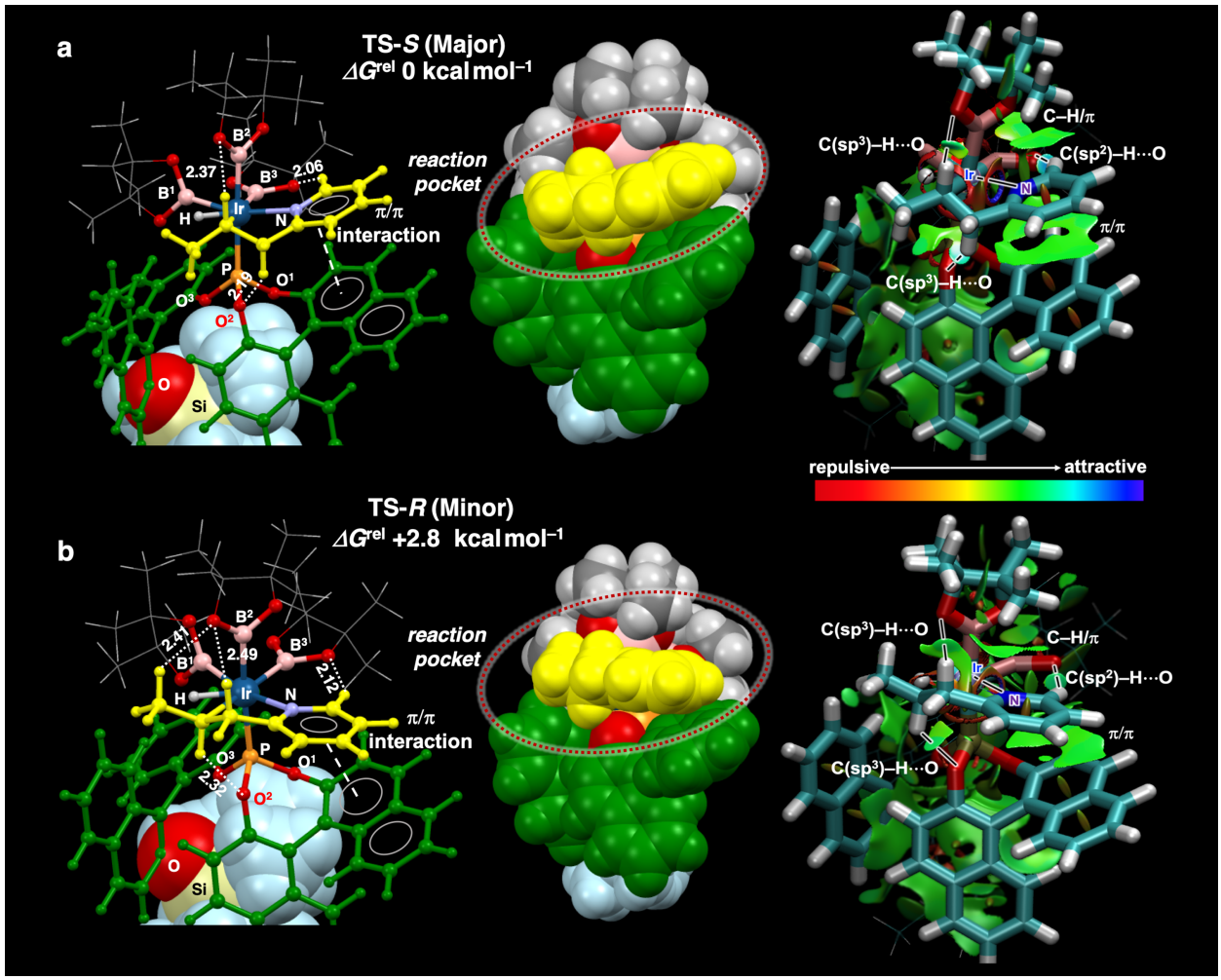

Figure 4. 3-D representations with geometrical features of the transition states leading to the major enantiomer (**TS-*S***) (a) and the minor enantiomer (**TS-*R***) (b). The binaphthyl moieties of **L6** are shown in green, the TIPS group in pale blue (^{i}Pr) and pale yellow (Si), and the substrate in yellow. All atomic distances are given in Å.

In summary, the asymmetric borylation of unactivated methylene C(sp^3)–H bonds was achieved with excellent enantioselectivity resulting from the efficient discrimination of enantiotopic C–H bonds by the catalyst. Crucial to the reactivity and enantioselectivity is the generation of a monophosphite-Ir-tris(boryl) complex that provides a narrow chiral reaction pocket conceptually analogous to an enzyme active site with the multiple secondary attractive interactions between the substrate and the catalyst.[14c] Further experimental work to expand the scope of asymmetric C–H borylation and more advanced computational studies to explore full catalytic cycles are in progress.

ASSOCIATED CONTENT

Supporting Information

Experimental procedures, the characterization of all new compounds, and details on the computational studies are provided in the Supplementary Information. The Supporting Information is available free of charge on the ACS Publications website.

AUTHOR INFORMATION

Corresponding Author

*sawamura@sci.hokudai.ac.jp; *smaeda@eis.hokudai.ac.jp

ACKNOWLEDGMENT

This work was supported by JST ACT-C Grant Number JPMJCR12YN, MEXT KAKENHI Grant Number JP15H05801 in Precisely Designed Catalysts with Customized Scaffolding, and JSPS KAKENHI Grant Number JP18H03906 in Grant-in-Aid for Scientific Research (A) to M. S. R. L. R. thanks MEXT for the

scholarship support during his Ph.D. studies. This research used computational resources provided by the Academic Center for Computing and Media Studies, Kyoto University. We thank FUJIFILM Wako Pure Chemical Corporation for providing Silica-SMAP used in the preparation of racemic products.

REFERENCES

(1) Reviews on enantioselective C–H functionalization: (a) Saint-Denis, T. G.; Zhu, R.-Y.; Chen, G.; Wu, Q.-F.; Yu, J.-Q. Enantioselective C(sp^3)–H bond activation by chiral transition metal catalysts. *Science* **2018**, *359*, eaao4798. (b) Newton, C. G.; Wang, S.-G.; Oliveira, C. C.; Cramer, N. Catalytic enantioselective transformations involving C–H bond cleavage by transition-metal complexes. *Chem. Rev.* **2017**, *117*, 8908–8976. (c) Lu, Q.; Glorius, F. Radical enantioselective C(sp^3)–H functionalization. *Angew. Chem. Int. Ed.* **2017**, *56*, 49–51.

(2) Selected examples of stereochemistry-generating C(sp^3)–H functionalization that caused desymmetrization of symmetrical molecules through differentiation of enantiotopic carbons: (a) He, J.; Shao, Q.; Wu, Q.; Yu, J.-Q. Pd(II)-catalyzed enantioselective C(sp^3)–H borylation. *J. Am. Chem. Soc.* **2017**, *139*, 3344–3347. (b) Fu, J.; Ren, Z.; Basca, J.; Musaev, D. G.; Davis, H. M. L. Desymmetrization of cyclohexanes by site- and stereoselective C–H functionalization. *Nature* **2018**, *564*, 395–399. (c) Milan, M.; Bietti, M.; Costas, M. Highly enantioselective oxidation of nonactivated aliphatic C–H bonds with hydrogen peroxide catalyzed by manganese complexes. *ACS Cent. Sci.* **2017**, *3*, 196–204. (d) Wasa, M.; Engle, K. M.; Lin, D. W.; Yoo, E. J.; Yu, J.-Q. Pd(II)-catalyzed enantioselective C–H activation of cyclopropanes. *J. Am. Chem. Soc.* **2011**, *133*, 19598−19601. (e) Xiao, K.-J.; Lin, D. W.; Miura, M.; Zhu, R.-Y.; Gong, W.; Wasa, M.; Yu, J.-Q. Palladium(II)-catalyzed enantioselective C(sp^3)–H activation using a chiral hydroxamic acid ligand. *J. Am. Chem. Soc*. **2014**, *136*, 8138−8142.

(3) (a) Pan, S.; Endo, K.; Shibata, T. Ir(I)-catalyzed enantioselective secondary sp^3 C–H bond activation of 2-(alkylamino)pyridines with alkenes. *Org. Lett.* **2011**, *13*, 4692–4695. (b) Pan, S.; Matsuo, Y.; Endo, K.; Shibata, T. Cationic iridium-catalyzed enantioselective activation of secondary sp^3 C–H bond adjacent to nitrogen atom. *Tetrahedron* **2012**, *68*, 9009–9015. (c) Tahara, Y.-K.; Michino, M.; Ito, M.; Kanyiva, K. S.; Shibata, T. Enantioselective sp^3 C–H alkylation of γ-butyrolactam by a chiral Ir(I) catalyst for the synthesis of 4-substituted γ-amino acids. *Chem. Comm*. **2015**, *51*, 16660–16663.

(4) (a) Zhang, F.-L.; Hong, K.; Li, T.-J.; Park, H.; Yu, J.-Q. Functionalization of C(sp^3)–H bonds using a transient directing group. *Science* **2016**, *351*, 252–256. (b) Wang, H.; Tong, H.-R.; He, G.; Chen, G. An enantioselective bidentate auxiliary directed Palladium-catalyzed benzylic C−H arylation of amines using a BINOL phosphate ligand. *Angew. Chem. Int. Ed.* **2016***, 55*, 15387–15391. (c) Murakami, R.; Sano, K.; Iwai, T.; Taniguchi, T.; Monde, K.; Sawamura, M. Palladium-catalyzed asymmetric C(sp^3)–H allylation of 2-alkylpyridines. *Angew. Chem. Int. Ed.* **2018**, *57*, 9465–9469.

(5) (a) Liao, K.; Negretti, S.; Musaev, D. G.; Bacsa, J.; Davies, H. M. L. Site-selective and stereoselective functionalization of unactivated C–H bonds. *Nature* **2016***, 533*, 230–234. (b) Liao, K.; Yang, Y.-F.; Li, Y.; Sanders, J. N.; Houk, K. N.; Musaev, D. G.; Davies, H. M. L. Design of catalysts for site-selective and enantioselective functionalization of nonactivated primary C–H bonds. *Nat. Chem.* **2018***, 10*, 1048–1055.

(6) (a) Chen, G.; Gong, W.; Zhuang, Z.; Andrä, M. S.; Chen, Y.-Q.; Hong, X.; Yang, Y. F.; Liu, T.; Houk, K. N.; Yu, J.-Q. Ligand-accelerated enantioselective methylene C(sp^3)–H bond activation. *Science* **2016**, *353*, 1023–1027. (b) Yan, S.-B.; Zhang, S.; Duan, W.-L. Palladium-catalyzed asymmetric arylation of C(sp^3)–H bonds of aliphatic Amides: Controlling enantioselectivity using chiral phosphoric amides/amines. *Org. Lett.* **2015**, *17*, 2458–2461. (c) Yan, S.-Y.; Han, Y.-Q.; Yao, Q.-J.; Nie, X.-L.; Liu, L.; Shi, B.-F. Palladium(II)-catalyzed enantioselective arylation of unbiased methylene C(sp^3)–H bonds enabled by a 1-pyridynylisopropyl auxiliary and chiral phosphoric acids. *Angew. Chem. Int. Ed.* **2018**, *57*, 9093–9097. (d) Han, Y.-Q.; Ding, Y.; Zhou, T.; Yan, S.-Y.; Song, H.; Shi, B.-F. Pd(II)-catalyzed enantioselective alkynylation of unbiased methylene C(sp^3)–H bonds using 3,3'-fluorinated-BINOL as a chiral ligand. *J. Am. Chem. Soc.* **2019**, *141*, 4558–4563.

(7) (a) Kawamorita, S.; Murakami, R.; Iwai, T.; Sawamura, M. Synthesis of primary and secondary alkylboronates through site-selective C(sp^3)–H activation with silica-supported monophosphine–Ir catalysts. *J. Am. Chem. Soc.* **2013**, *135*, 2947–2950. (b) Murakami, R.; Tsunoda, K.; Iwai, T.; Sawamura, M. Stereoselective C–H borylations of cyclopropanes and cyclobutanes with silica-supported monophosphane-Ir catalysts. *Chem. Eur. J.* **2014**, *20*, 13127–13131. (c) Murakami, R.; Iwai, T.; Sawamura, M. Site-selective and stereoselective C(sp^3)–H borylation of alkyl side chains of 1,3-azoles with a silica-supported monophosphine-Iridium catalyst. *Synlett* **2016***, 27*, 1187–1192.

(8) Reyes, R. L.; Harada, T.; Taniguchi, T.; Monde, K.; Iwai, T.; Sawamura, M. Enantioselective Rh- or Ir-catalyzed directed C(sp^3)–H borylation with phosphoramidite chiral ligands. *Chem. Lett.* **2017**, *46*, 1747–1750.

(9) Zou, X.; Zhao, H.; Li, Y.; Gao, Q.; Ke, Z.; Xu, S. Chiral bidentate boryl ligand enabled iridium-catalyzed asymmetric C(sp^2)–H borylation of diarylmethylamines. *J. Am. Chem. Soc*. **2019**, *141*, 5334–5342.

(10) (a) Gavrilov, K. N.; Lyubimov, S. E.; Petrovskii, P. V.; Zheglov, S. V.; Safronov, A. S.; Skazov, R. S.; Davankov, V. A. Facile one-pot synthesis of BINOL- and H_8-BINOL-based aryl phosphites and their use in palladium catalyzed asymmetric allylation. *Tetrahedron* **2005**, *61*, 10514–10520. (b) Gavrilov, K. N.; Zheglov, S. V.; Gavrilova, M. N.; Novikov, I. M.; Maksimova, M. G.; Groshkin, N. N.; Rastorguev, E. A.; Davankov, V. A. Phosphites and diamidophosphites based on mono-ethers of BINOL: a comparison of enantioselectivity in asymmetric catalytic reactions. *Tetrahedron* **2012**, *68*, 1581–1589. (c) Gavrilov, K. N.; Lyubimov, S. E.; Zheglov, S. V.; Benetsky, E. B.; Petrovskii, P. V.; Rastorguev, E. A.; Grishina, T. B.; Davankov, V. A. MOP-type binaphthyl phosphite and diamidophosphite ligands and their application in catalytic asymmetric transformations. *Adv. Synth. Catal.* **2007***, 349*, 1085–1094.

(11) The use of one equivalent of the substrate **1a** in the presence of 2,6-lutidine (100 mol%) similarly gave the product at 73% (^{1}H NMR) and 98% ee. However, the use of stoichiometric amount of 2,6-lutidine led to difficulty in product purification.

(12) See Supporting Information for details of effects of the additive and the use of the excess substrate.

(13) Rendler, S.; Plefka, O.; Karatas, B.; Auer, G.; Fröhlich, R.; Mück-Lichtenfeld, C.; Grimme, S.; Oestreich, M. Stereoselective alcohol silylation by dehydrogenative Si–O coupling: scope, limitations, and mechanism of the Cu-H-catalyzed non-enzymatic kinetic resolution with silicon-stereogenic silanes. *Chem. Eur. J.* **2008**, *14*, 11512–11528.

(14) In previous theoretical studies, the C–H activation step was shown to be the rate-determining step. See (a) Tamura, H.; Yamazaki, H.; Sato, H.; Sakaki, S. Iridium-catalyzed borylation of benzene with diboron. Theoretical elucidation of catalytic cycle including unusual iridium(V) intermediate. *J. Am. Chem. Soc.* **2003**, *125*, 16114–16126. (b) Huang, G.; Kalek, M.; Liao, R.-Z.; Himo, F. Mechanism, reactivity, and relectivity of the iridium-catalyzed C(sp^3)–H borylation of chlorosilanes. *Chem. Sci.* **2015**, *6*, 1735–1746. (c) Haines, B. E.; Saito, Y.; Segawa, Y.; Itami, K.; Musaev, D. G. Flexible reaction pocket on bulky diphosphine−Ir complex controls regioselectivity in para-selective C−H borylation of arenes. *ACS Catal.* **2016**, *6*, 7536−7546. See also ref. 9.

(15) Maeda, S.; Harabuchi, Y.; Takagi, M.; Taketsugu, T. Morokuma, K. Artificial force induced reaction (AFIR) method for exploring quantum chemical potential energy surfaces. *Chem. Rec.* **2016**, *16*, 2232–2248.

(16) Sameera, W. M. C.; Maeda, S.; Morokuma, K. Computational catalysis using the artificial force induced reaction method. *Acc. Chem. Res.* **2016**, *49*, 763–773.

(17) At obtained stationary structures, Gibbs free energy values were estimated through the harmonic vibrational analysis, where all frequencies below 50 cm^{-1} were replaced by 50 cm^{-1}, see: Ryu, H.; Park, J.; Kim, H. K.; Park, J. Y.; Kim, S.-T.; Baik, M.-H. Pitfalls in computational modeling of chemical reactions and how to avoid them. *Organometallics* **2018**, *37*, 3228−3239.

(18) A computationally estimated product enantiomer ratio is *S*/*R* 77:23 when all of the examined twelve TSs are considered. This population is in accord with the trend of the reaction favoring the *S* isomer, while not matching quantitatively to the experimental value.
(19) Johnston, R. C.; Cheong, P. H.-Y. C–H···O non-classical hydrogen bonding in the stereomechanics of organic transformations: theory and recognition. *Org. Biomol. Chem.* **2013**, *11*, 5057–5064.
(20) Ishii, T.; Ryo, W.; Moriya, T.; Ohmiya, H.; Mori, S.; Sawamura, M. Cooperative catalysis of metal and O–H···O/sp^3-C–H···O two-point hydrogen bonds in alcoholic solvents: Cu-catalyzed enantioselective direct alkynylation of aldehydes with terminal alkynes. *Chem. Eur. J.* **2013***, 19*, 13547–13553.
(21) Schwarzer, M. S.; Fujioka, A.; Ishii, T.; Ohmiya, H.; Mori, S.; Sawamura, M. Enantiocontrol by assembled attractive interactions in copper-catalyzed asymmetric direct alkynylation of α-ketoesters with terminal alkynes: OH···O/sp^3-CH···O two-point hydrogen bonding combined with dispersive attractions. *Chem. Sci.* **2018**, *9*, 3484–3493.
(22) Johnson, E.R.; Keinan, S.; Mori-Sánchez, P.; Contreras-García, J.; Cohen, A. J.; Yang, W. Revealing noncovalent interactions. *J. Am. Chem. Soc.* **2010**, *132*, 6498–6506.
(23) Humphrey, W.; Dalke, A.; Schulten, K. VMD - Visual molecular dynamics. *J. Molec. Graphics* **1996**, *14*, 33–38.

For Table of Contents (TOC) Only